

# ULTIMATE LIMIT STATE ASSESSMENT OF STIFFENED PANEL STRUCTURES FOR VERY LARGE ORE CARRIER VIA NONLINEAR FINITE ELEMENT METHOD

HUNG-CHIEN DO<sup>1</sup>, WEI JIANG<sup>2</sup>, JIANXIN JIN, XUEDONG CHEN

1 State Key Laboratory of Digital Manufacturing Equipment and Technology, Huazhong University of Science and Technology, Wuhan, Hubei, 430074, P.R. China

<sup>1</sup> dhchienvn@hotmail.com , <sup>2</sup>jiangw@hust.edu.cn

## **ABSTRACT**

*Reduces weight of hull structures designed for a very large carrier plays an important role as the economic efficiency is the most significant aspect. It is known that the traditional allowable working stress approaches with high safety and reliability, it means that the hull structural weight is higher than the actual requirement in operation. Recently, the limit state approach has been widely applied for analysis and assessment of marine structures, the limit strength of structures is determined by nonlinear finite element analysis (FEA) method. A Very Large Ore Carrier (VLOC) is designed by using IACS Common Structural Rules (CSR) method in this article, and pre-CSR method is adopted to improve cross-sectional of the bottom and deck structures. Given that the stiffened panel under the combination of axial or biaxial compression and lateral pressure loads for computation, ultimate strength of the ship structures designed by using the aforementioned method are analyzed by using the nonlinear finite element method (FEM). The results show that the difference of ultimate strength of ship structures designed by using pre-CSR method and CSR method is able to neglect. It can be seen that the weight of hull structure can be reduced by 0.56 percent (640 tons in this case) without reducing ultimate strength when pre-CSR method is applied.*

## **KEYWORDS**

*Ultimate limit state (ULS); stiffened panel; Very Large Ore Carrier; Nonlinear FEA; pre-CSR method; CSR method*

## **1. INTRODUCTION**

A stiffened panel is basically an assembly of the support member and plate elements in ship hull structures. An estimation of ultimate strength of these elements plays an important role in high safety, reliability and economics of design structures [1]. In the marine industry, ultimate strength has been widely applied as one of the basics of structures in design and assessment; it is shown in many literatures of some organizations such as International Organization for Standardization (ISO), International Maritime Organization (IMO), International Ships and Offshore Structures Congress (ISSC), International Association of Classification Societies (IASC) [2], Classification Societies of each country [3]. These organizations have proposed standards to simply, quickly and directly determine the limit states. Generally, the limit states involve four types, namely serviceability limit state (SLS) - displacement and deflections, ultimate limit state (ULS) - ultimate strength behavior, fatigue limit state (FLS) - fatigue and fracture behaviors, and accidental limit states (ALS) - collision, fire, blast, dropped objects, etc.

Concerning Finite Element Method (FEM), there are many advantages in analyzing structural problems such as stress, strain, and vibration [4-6], the ULS approach to design has been mostly applied by using nonlinear FEM with the help of powerful computer. In this paper, we focus on ULS for assessment of ship hull structures based on nonlinear Finite Element Analysis (FEA), e.g. ANSYS, following the guiders of the IACS common structural rules (CSR) and reference to American Bureau of Shipping (ABS) rules. The plating and stiffeners design are taken into account by using a Very Large Ore Carrier (VLOC) and then being in the performance of nonlinear FEA.

In general, in both large ship and VLOC, the structures are usually designed with a longitudinal framing system (combined with longitudinal stiffeners, girders and transverse floors). When a ship bending in hogging and sagging, the bottom and deck structures are compressed along the edges, according to the properties of each structural area, stiffened panels surrounded by the support members subjected to combined axial or biaxial compression and lateral pressure loads. The magnitude of lateral pressure depends on draft of each loading condition, density of water area in ship operation. In computation, these conditions are considered in stiffened panel model, the results obtained by ANSYS nonlinear FEA of ultimate strength in various conditions of stiffened panel in the bottom and deck for both CSR and pre-CSR methods are compared to each other, and they are also compared with adopted literatures[7, 8].

## **2. METHODOLOGY AND NUMERICAL MODEL**

### **2.1. Ultimate limit state assessment method**

Related to the present studies for ULS assessment of the structural stiffened panel, two methodological groups are proposed as follows.

Design group: By applying rules (IACS and ABS rules), CSR plating and stiffener structures are quickly designed and pre-IACS CSR structures are improved for hypothetical VLOC cargo hold area stiffened panel structures.

Evaluation group: Nonlinear FEA ANSYS is utilized to estimate the performance of the results of CSR and pre-CSR models by employing these models with various loading and boundary conditions, firstly with linear FEM analysis to determine buckling status and secondly with nonlinear analysis to behave ultimate strength.

It is known that, ship design structures are very complicated, specially, with a VLOC, it requires designers not only to have good background in hydrostatic, wave theory, and mechanic but also to be an experienced specialist. Since the rules of ship design structures have been proposed, the design of ship working is easier according to rule requirements, the designers can quickly calculate, determine and choose a model structure complying with the type of ship, the requirements from ship owner and manufactures. When the rules are employed, ship structures have high safety factors, and in the local structures, it is not detailed suitable for agreement structure areas [2, 3]. There are many authors study how to improve the rules, to change the concepts of high safety factors for material saving. In other words, reduction in ship light weight is equivalent to increasing the dead weight and the economic efficiency.

In design group, firstly, plating and stiffeners in both outer bottom and inner bottom, and deck are determined, namely CSR model. Secondly, the authors impose a new model based on CSR model, namely pre-CSR model [9]. Consider the marginal values of corrosion, stiffened panel designed by the rules, CSR model is compared to pre-CSR model under the following conditions,

- 2.5-4.0 mm increase of outer bottom plate thickness as ultimate limit state;
- 15% increase of stiffened panel bottom and deck modulus with effective width under local pressure.
- 2-5 mm increase of weather deck plate thickness with modulus and fatigue requirements;
- 1 mm increase of inner bottom plate thickness with local pressure actions.

In the evaluation group, both CSR and pre-CSR models will be analyzed in linear and nonlinear with FEM, ANSYS code is a tool which is useful for mechanical fracture, it depends on meshing model, initial deflection, constrained boundary, and applied loads. In addition, nonlinear analysis also requires a powerful computer to meet long computation time. Following the results of linear and nonlinear analyses, buckling status and ultimate limit state of stiffened structures will be determined to compare the CSR model to pre-CSR model.

## 2.2. Object ship particular

For convenience, a Very Large Ore Carrier (VLOC) of 380,000 DWT is undertaken to analysis her stiffened panel, particular as shown in Table 1.

Table 1. Principal dimensions of hypothetical object ship

| Item                         | Magnitude |
|------------------------------|-----------|
| Length scantling, $L_s$ [m]  | 360.000   |
| Breadth, $B$ [m]             | 65.000    |
| Depth, $D$ [m]               | 30.000    |
| Designed draught, $d$ [m]    | 21.500    |
| Scantling draught, $d_s$ [m] | 23.000    |
| Block coefficient, $C_B$     | 0.870     |

## 2.3. Material and properties of stiffened panel model.

Generally, ship structural design usually uses mild steel, but to reduce ship light weight, high tensile steel is employed. In addition, for ship design structures, the material of plates often differs from that of stiffeners. For example, the plates are made of mild steel, yield stress  $\sigma_{yp}$ , while the stiffeners are made of high-tensile steel, yield stress  $\sigma_{ys}$ . Meanwhile, the values of Young's modulus  $E$  or the values of Poisson's ratio  $\nu$  are the same in these two types of material. Hence, an equivalent value of the material yield stress for a plate-stiffeners combination parameter  $\sigma_{yeq}$  is frequently used to represent the yield stress of the entire panel, given by

$$\sigma_{yeq} = \frac{Bt\sigma_{yp} + n_s(h_w t_w + b_f t_f)\sigma_{ys}}{Bt + n_s(h_w t_w + b_f t_f)} \quad (1)$$

Where,  $B$  is the distance between two strength girders, other parameters are shown in Table 2. When taking a single stiffener with its attached plate analysis as column buckling, from the equation(1), the equivalent yield stress is defined as follows

$$\sigma_{y_{eq}} = \frac{bt\sigma_{yp} + (h_w t_w + b_f t_f)\sigma_{ys}}{bt + (h_w t_w + b_f t_f)} \quad (2)$$

For convenient analysis of a hypothetical ship object but without the loss of generality, the outer bottom stiffened-plate structures are designed with the same material parameters, thus we have  $\sigma_{y_{eq}} = \sigma_{yp} = \sigma_{ys} = \sigma_Y = 355$  MPa. In the scope of this study, the entire structural ship is made of 36AH high tensile steel with yield stress  $\sigma_Y$  of 355 MPa, Young's modulus  $E$  of 205.8 GPa, and Poisson's ratio  $\nu$  of 0.3.

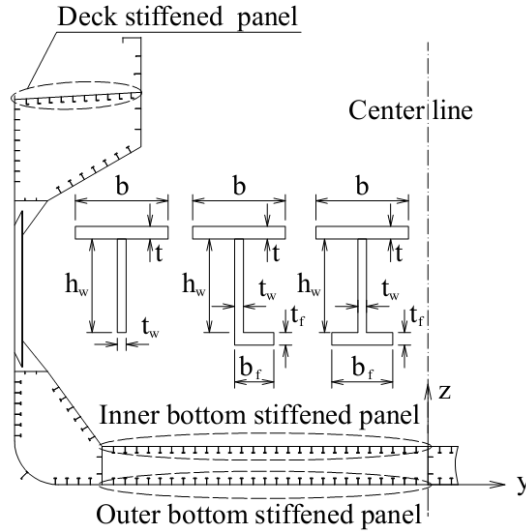


Figure 1. Mid-ship section and 3 types of stiffener

According to results of the design group, plating and stiffeners properties are determined comply with IASC CSR and ABS rules. In Table 2,  $a$ ,  $b$ ,  $n_s$ , and  $t$  are the length of stiffeners (the distance between two strength girders), the breadth of plating between longitudinal stiffeners, the number of longitudinal stiffeners, and the thickness of plates, respectively;  $h_w$ ,  $t_w$ ,  $b_f$  and  $t_f$  are high of web plates, the thickness of web plates, the breadth of flange plates, and the thickness of flange plates, respectively. Concerning ship and offshore structures, there are three popular types of stiffeners as illustrated in Figure 1, namely, flat bar, angle stiffener, and T-type. In the present study, the stiffened panel on outer bottom and inner bottom with T-type longitudinal stiffeners is analyzed under biaxial compression and lateral pressure. On the deck structures, stiffeners with both T type and L type are employed in order to estimate which type is better. The slenderness ratio  $\beta = b/t \sqrt{\sigma_{yp}/E}$  of the bottom plating is in the range of [1.99, 4.45] and the deck plates are in the range of [2.36, 2.55].

The nomenclature stiffened panel structures are analyzed as shown in Figure 2. The potential load components of loading on a stiffened panel generally are categorized into the six types, as follows [10, 11],

- (1) Longitudinal axial load in the  $x$  direction;
- (2) Transverse axial load in the  $y$  direction;
- (3) Edge shear stress;
- (4) Longitudinal in-plane bending moment in the  $x$  direction;

- (5) Transverse in-plane bending moment in the  $y$  direction;
- (6) Lateral pressure.

Table 2. Geometric properties of the cargo hold area stiffened panels

| Local       | Items   | $a$ [mm] | $b$ [mm] | $n_s$ | $t$ [mm] | $h_w$ [mm] | $t_w$ [mm] | $b_f$ [mm] | $t_f$ [mm] |
|-------------|---------|----------|----------|-------|----------|------------|------------|------------|------------|
| OB          | Pre-CSR | 3500     | 915      | 27    | 18.53    | 420        | 10         | 172        | 16         |
|             | CSR     | 3500     | 915      | 27    | 21.80    | 470        | 10         | 162        | 16         |
| IB          | Pre-CSR | 3500     | 915      | 27    | 14.64    | 420        | 10         | 146        | 16         |
|             | CSR     | 3500     | 915      | 27    | 15.64    | 440        | 10         | 156        | 16         |
| DK L/T-type | Pre-CSR | 3500     | 915      | 10    | 13.38    | 350        | 10         | 142        | 15         |
|             | CSR     | 3500     | 915      | 10    | 14.38    | 380        | 10         | 144        | 16         |

\*Note: OB = Outer bottom, IB = Inner bottom, DK L/T-type = Deck with L-type of stiffeners and Deck with T-type of stiffeners.

In this regard, some of combined acting load are depending on the collapse mode to develop the ultimate strength formulations for the panel. These are illustrated in the following using the nomenclature of Figure 2, where  $\sigma_{xav}$  is the average axial stress in the  $x$  direction,  $\sigma_{yav}$  is the average axial stress in the  $y$  direction,  $\sigma_{av}$  is the average edge shear stress and  $p$  is the lateral pressure. Note that in the  $x$  direction,  $\sigma_{x2}$  is always the larger edge stress than  $\sigma_{x1}$  [1].

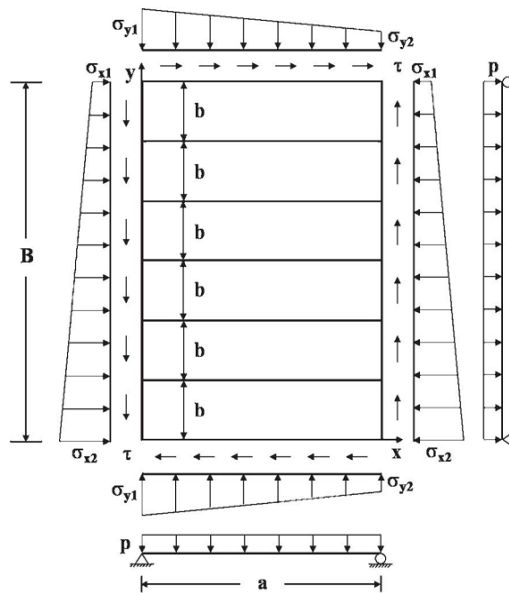


Figure 2. Stiffened plate structures under combined loads

Model structures after being designed are computed and analyzed by ANSYS nonlinear FEA as shown in Figure 2, effect factors of resultant accuracy are initial deflection, residual stresses. Although it is known that the welding residual stresses generally reduce the local buckling strength of a stiffened plate, welding residual stresses may also develop in both the longitudinal and transverse directions because the support members are usually attached by welding in these two directions, the magnitude of residual stresses in this study is often very small, it can be ignored [12]. The initial deflection of plating (between support members) and stiffeners web are assumed as below,

$$w_{opl} = \frac{b}{200} \quad (3)$$

$$w_{oc} = w_{os} = \frac{a}{1000} \quad (4)$$

Where,  $w_{opl}$ ,  $w_{oc}$ , and  $w_{os}$  are the maximum plate initial deflection, the stiffener in the vertical direction at column type initial deflection and the stiffener in the horizontal direction at side way initial deflection, respectively. They are obtained by these equations as follow

$$w_{opl} = A_0 \sin \frac{m\pi x}{a} \sin \frac{\pi y}{b} \quad (5)$$

$$w_{oc} = B_0 \sin \frac{\pi x}{a} \sin \frac{\pi y}{b} \quad (6)$$

$$w_{os} = C_0 \sin \frac{z}{h_w} \sin \frac{\pi x}{a} \quad (7)$$

Where  $m$  is buckling half-wave number in  $x$ -direction;  $A_0$ ,  $B_0$ , and  $C_0$  are the amplitude of the deflection function;  $h_w$  is the stiffener web height which excluding stiffener flange thickness.

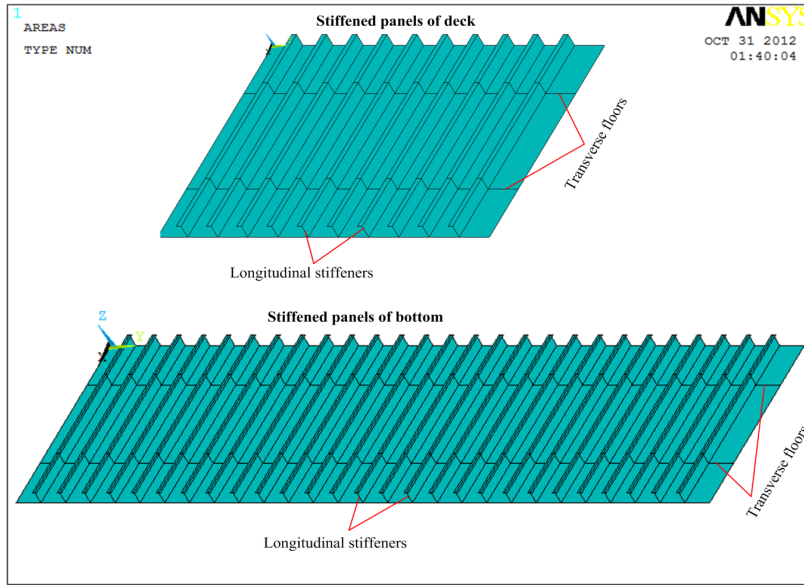


Figure 3. Numerical of deck and bottom stiffened panels for Nonlinear FEA

A pseudo-ultimate strength  $\sigma_{xu}$  along  $x$  direction can be obtained by the Johnson-Ostenfeld formula as a plasticity correction of the elastic buckling stress, as follows.

$$\sigma_{xu} = \begin{cases} \sigma_{xE} & \text{for } \sigma_{xE} \leq 0.5\sigma_{Yeq} \\ \sigma_{Yeq} \left( 1 - \frac{\sigma_{Yeq}}{4\sigma_{xE}} \right) & \text{for } \sigma_{xE} > 0.5\sigma_{Yeq} \end{cases} \quad (8)$$

Where,  $\sigma_{xE}$  is the elastic buckling stress. Based on equation(8), the pseudo-ultimate strength  $\sigma_{yu}$  along  $y$  direction can be simply determined by substituting  $x$  for  $y$ , both of  $\sigma_{xE}$  and  $\sigma_{yE}$  can be

obtained by base-experienced formulae, and they are obtained by resultant ANSYS FEA in this paper.

When stiffened panel under axial compressive load, ultimate stress can be also determined by the Paik-Thayamballi empirical formula method, as follows,

$$\frac{\sigma_{xu}}{\sigma_{yeq}} = \frac{1}{\sqrt{0.995 + 0.936\lambda^2 + 0.170\beta^2 + 0.188\lambda^2\beta^2 - 0.067\lambda^4}} \quad (9)$$

Where,

$$\lambda = \frac{a}{\pi r} \sqrt{\frac{\sigma_{yeq}}{E}}, \quad \beta = \frac{b}{t} \sqrt{\frac{\sigma_{yp}}{E}}, \quad r = \sqrt{\frac{I}{A_s}}, \quad A_s = bt + h_w t_w + b_f t_f,$$

$$I = \frac{bt^3}{12} + bt \left( z_0 - \frac{t}{2} \right)^2 + \frac{h_w^3 t_w}{12} + h_w t_w \left( z_0 - t - \frac{h_w}{2} \right)^2 + \frac{b_f t_f^3}{12} + b_f t_f \left( t + h_w + \frac{t_f}{2} - z_0 \right)^2, \quad (10)$$

$$z_0 = \frac{0.5bt^2 + h_w t_w (t + 0.5h_w) + b_f t_f (t + h_w + 0.5t_f)}{bt + h_w t_w + b_f t_f}$$

In combination of formulae(10),  $\lambda$  is the slenderness coefficient of column;  $\beta$  is the slenderness coefficient of plating;  $r$  is radius of gyration;  $A_s$  is cross section area;  $I$  is the inertial moment of cross-section;  $z_0$  is distance between  $x$  axis and neutral axis of cross-section;  $b$  is the effective breadth;  $t$ ,  $t_w$  and  $t_f$  are the thickness of plating, web plate and flange plate, respectively;  $h_w$  is height of web plate and  $b_f$  is the breadth of flange plate, they are illustrated in Figure 4.

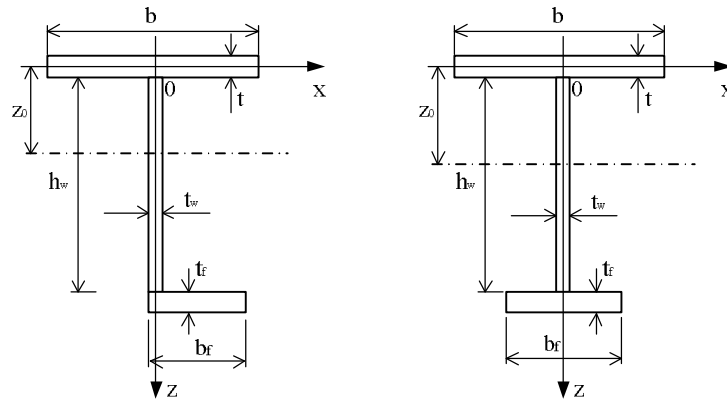


Figure 4. Nomenclature of cross-sections

## 2.4. Boundary condition

In the present study, two-bay model uses simply supported boundary condition along the girder or longitudinal edges[13-15], in Committee III.1 of 17<sup>th</sup> and 18<sup>th</sup> ISSC (International Ships and Offshore Structures Congress) [16, 17], the considered two-bay model is better than one-bay model in the pre-buckling phase and displays a greater decrease of strength after buckling. The boundary conditions are applied,  $T[x,y,z]$  and  $R[x,y,z]$  represent translational constraints and rotational constraints related to  $x$ -,  $y$ -, and  $z$ -coordinates, respectively. The values of  $x$ ,  $y$ , and  $z$  are either “1” or “0”. A “1” means “without constraint” and a “0” indicates “with constraint”, is shown in Figure 5.

Generally, simple supported and clamped boundary condition in the ultimate limit state assessment are adopted, however, when compressive loads in  $x$  direction are predominant the effect of the two boundary conditions is negligible. Also, the boundary conditions at longitudinal edges play a significant role when transverse axial compressive loads are predominant. In order to convenient for calculation as well as assessment of ultimate strength structures, in this regards, simple supported is applied because longitudinal axial compressive loads are predominant for both of deck and bottom structures, as follows,

- Simply supported at A-C and A'-C': T[1,1,0] and R[1,0,0], each edge having equal  $y$ -displacement;
- At transverse floors: T[1,1,0] for plate nodes, and T[1,0,1] for stiffener web nodes;
- Symmetric condition at A-A': R[1,0,0] with all plate nodes and stiffener nodes having an equal  $x$ -displacement; Symmetric condition at C-C': T[0,1,1] and R[1,0,0].

## 2.5. Loading conditions

In Figure 5 (a), both of outer and inner bottoms are under combined biaxial compression with the loading ratio:  $\sigma_x:\sigma_y$ , meanwhile on the deck, only an axial load along  $x$  direction edges is applied as illustrated in Figure 5 (b). For outer bottom stiffened panel, the extreme of hydrostatic pressure (lateral pressure  $p$ ) to the outer bottom of the object is  $p = 0.23$  maps by using the formulae of IASC CSR, lateral pressures can be determined with inner bottom  $p = 0.359$  MPa and with weather deck  $p = 0.034$  MPa .

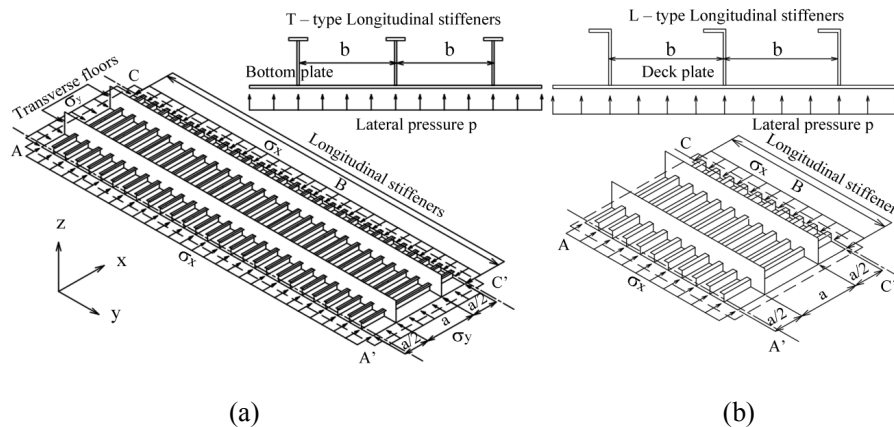


Figure 5. Nonlinear FEA model of the stiffened panel surrounded by supporting members

Firstly, stiffened panels under compressive without lateral pressure by performing ANSYS nonlinear finite element analysis, these are suitable ship in dry-dock, i.e., stiffened panel on deck structures under axial compressive load, it means that  $\sigma_x:\sigma_y = 1:0$ , while outer bottom and inner bottom under biaxial of ratio  $\sigma_x:\sigma_y = 0.79:0.21$ .

Secondly, in case of ship operation, under hydrostatic pressure in water acting outer bottom which depends on density of water and draft of ship, with cargo hold is full load active inner bottom, the effects of the weather pressures active on the deck structures, where lateral pressure  $p$  is applied.

## 2.6. Meshing model

By performance of FEM, the accuracy and speed of computation can be defined by the number of finite elements. In the approved documents of Committee III.1 of 17<sup>th</sup>, for the outer/inner bottom plates and deck plates, the number of plate-shell elements along the breadth direction  $b$  and the



length direction  $a$  are 10 and 40, respectively. In Figure 6, for the stiffener web in the height direction and the flange in the breadth direction, the number of plate-shell elements is 6 and 4, respectively [16].

Concerning meshing model, on the deck structures, the number of element for stiffened panel is 16800 elements for L-types and T-types, meanwhile in the outer and inner bottom there are 44000 elements. Both elements of deck and bottom structure are SHELL 181. This is work done on personal computer: AMD Phenom II, X6 1055T, processor 2.8 GHz, RAM 12BG; each case takes several minute for linear analysis and several hours for nonlinear analysis, total of 16 cases in this study.

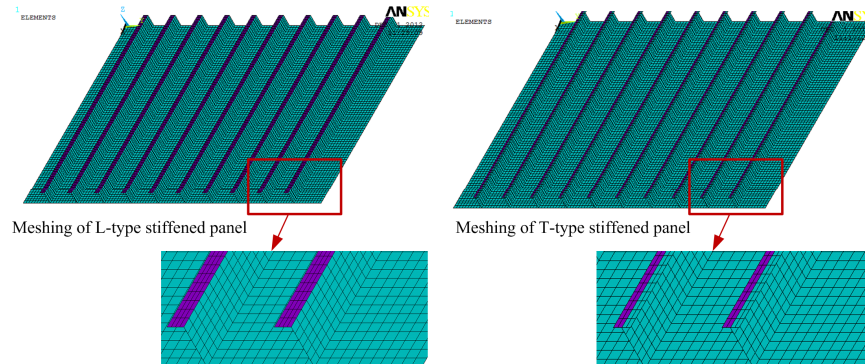


Figure 6. Meshing stiffened panels

### 3. RESULTS AND DISCUSSION

#### 3.1. Ultimate strength of deck stiffened panels.

In the deck structures, stiffeners consist of 2 types: L-type and T-type; the thickness and the other dimension of deck-plates, i.e. web and flange plates are the same. The aim of this application is to determine the difference of ultimate strength between two stiffener types. The stiffener dimension of the pre-CSR panel is  $h_w \times t_w = 350 \times 10$  mm, and  $b_f \times t_f = 14 \times 15$  mm. Concerns CSR panel, the stiffener dimension  $h_w \times t_w = 380 \times 10$  mm, and  $b_f \times t_f = 144 \times 16$  mm.

It is clear that the Nonlinear FEA is better than Paik-Thamballi formula, i.e. 8.64 - 10.95 percent of SCR models and 12.70-15.33 percent for pre-CSR models. An advantage of empirical formulae is helping designer determine the ultimate strength of structures quickly in preliminary structural design. However, the reliability of accurate results is not high, so the economic benefit will be lower than modern applications especially nonlinear finite element analysis. The ultimate strengths of L-type in this study are shown in Figure 8, the results of T-type deck structural stiffeners are shown in Figure 9.

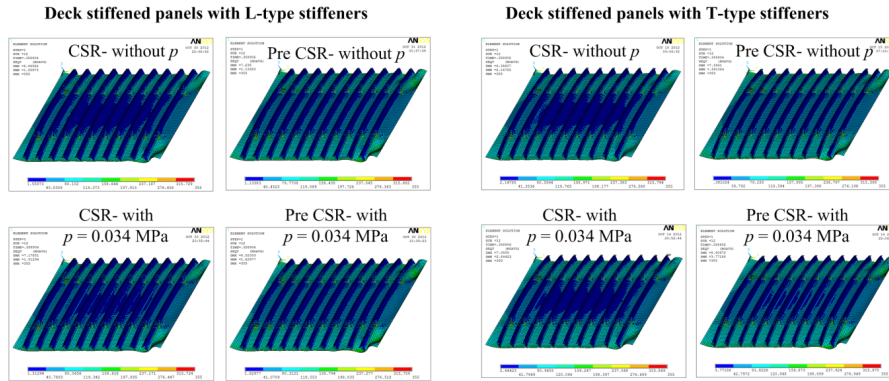


Figure 7. Deformed shapes and von-Mises stress distributions of CSR and pre-CSR deck model (amplification factor of 50)

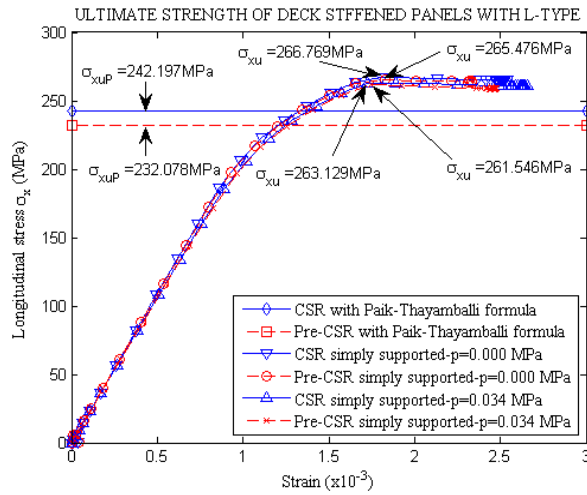


Figure 8. Ultimate strength of the deck-stiffened panels with L – type under axial loads

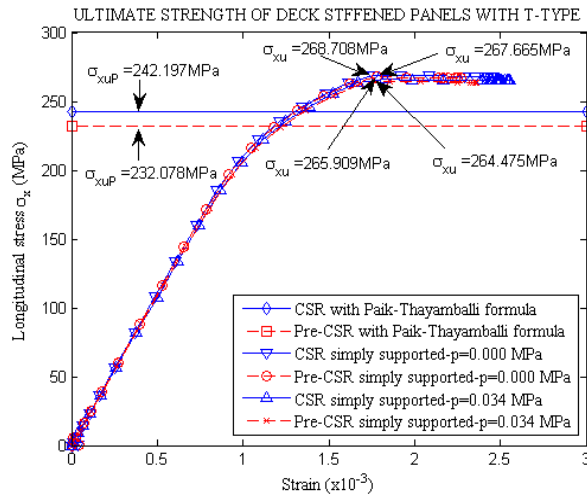


Figure 9. Ultimate strength of the deck-stiffened panels with T – type under axial loads

By applying nonlinear FEA, the ultimate stress of deck stiffened panel T-type outperforms L-type, i.e. about 0.73-1.06 percent and 0.82-1.12 percent of CSR models and pre-CSR models, respectively. It is clear that, the difference of these results is insignificant. Addition, with T-type, the ultimate strength is higher than with L-type. Actually, T-type is often existing residual welding stress; L-type is popularly used in stiffeners structures. The results of ultimate limit state of the deck stiffened plates are illustrated in Figure 7, which are obtained by ANSYS nonlinear finite element analysis. In ship structural design, following these results, deck stiffened panels of L-type and T-type can be also applied. The results of ultimate strength are obtained by differential methods as shown in Table 3.

Table 3. Ultimate strength of deck stiffened panels

| Design      | Method  |   |   |   |   |   |  |
|-------------|---|---|---|---|---|---|--|
|             | $\sigma_{xu}$ (MPa)<br>L-type<br>without<br>$p$ | $\sigma_{xu}$ (MPa)<br>L-type<br>with $p = 0.034$ Mpa | $\sigma_{xu}$ (MPa)<br>T-type<br>without<br>$p$ | $\sigma_{xu}$ (MPa)<br>T-type<br>with $p = 0.034$ Mpa | $\sigma_{xup}$ (MPa)<br>by<br>Paik's<br>formula | $\sigma_{xup}$ (MPa)<br>by<br>Paik's<br>FEA | $\sigma_{xup}$ (MPa)<br>by<br>Paik's<br>ALPS/<br>ULSAP |
| Pre-CSR     | 265.476   | 261.546   | 267.665   | 264.475   | 232.078   | 246.630                                     | 241.600  |
| CSR         | 266.769   | 263.129   | 268.708   | 265.909   | 242.197   | 252.270                                     | 243.370  |
| CSR/pre-CSR | 1.005   | 1.006   | 1.004   | 1.005   | 1.044   | 1.023                                       | 1.007  |

### 3.2 Ultimate strength of bottom stiffened panels.

According to bottom stiffened panels, both of CSR and pre-CSR model are under biaxial compressive loads with ratio  $\sigma_x : \sigma_y = 0.79 : 0.21$  which occurs in the design hull girder loading condition of the object ship, and the design lateral pressure load is  $p = 0.23$  MPa for outer bottom and  $p = 0.359$  MPa for inner bottom [18]. The number of bottom longitudinal stiffeners is 27 with T type. With the nomenclature of Figure 4 and data in the Table 2, in the outer bottom, the stiffener dimension of the pre-CSR panel is  $h_w \times t_w = 420 \times 10$  mm, and  $b_f \times t_f = 172 \times 16$  mm. Additional, the stiffener dimension of the CSR panel is  $h_w \times t_w = 470 \times 10$  mm, and  $b_f \times t_f = 162 \times 16$  mm. In inner bottom, the stiffener dimension of the pre-CSR panel is  $h_w \times t_w = 420 \times 10$  mm, and  $b_f \times t_f = 142 \times 16$  mm. Also, the stiffener dimension of the CSR panel is  $h_w \times t_w = 440 \times$

10 mm, and  $b_f \times t_f = 156 \times 16$  mm. In case without lateral pressure, ultimate stress is a small difference, i.e. about 0.23 - 0.35 percent.

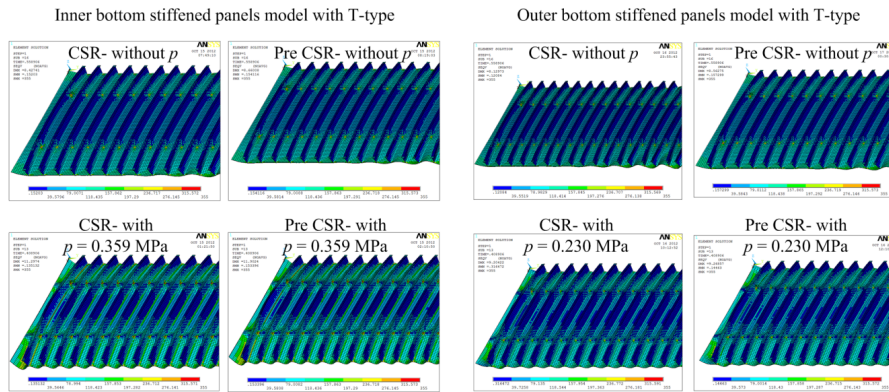


Figure 10. Deformed shapes and von-Mises stress distributions of CSR and pre-CSR bottom model (amplification factor of 50)

When applying lateral pressures, the ultimate stress of pre-CSR model is higher than that of CSR model, i.e. 0.35 - 2.91 percent and 0.23 - 2.50 percent for inner bottom and outer bottom, respectively. The reason is that by using appropriate design of pre-CSR stiffened structures, the bottom structural weight reduces and the ultimate strength increases. It is clear that, the lateral pressure play a significant role in ultimate strength of the panel structures.

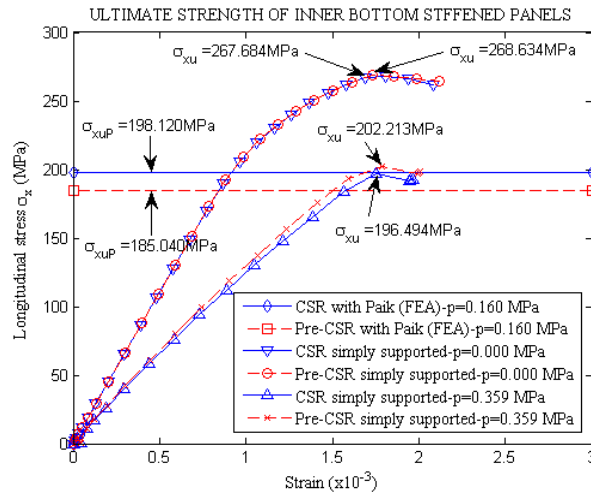


Figure 11. Ultimate strength of the inner bottom-stiffened panels under biaxial loads

In Figure 11, considering the pre-CSR model, the difference the ultimate strength is 9.28 percent in the inner bottom stiffened panel, and in the outer bottom, as shown in Figure 12, the ultimate stress in the present study is 26.41 percent higher than Paik's result.

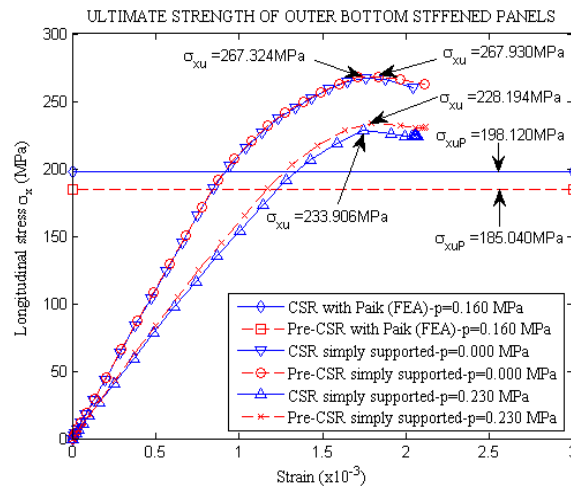


Figure 12. Ultimate strength of the outer bottom-stiffened panels under biaxial loads

These results are also compared to ultimate limit state performance of an AFRAMAX double hull oil tanker structures as shown in Table 4 and Figure 10, Paik [9] used Nonlinear FEA ANSYS, the material of the hull structures is the high tensile steel with the yield stress  $\sigma_y = 315$  MPa, the elastic modulus is  $E = 205.8$  GPa and Poisson's ratio is  $\nu = 0.3$ . Summarize of applied material aspect, in the present study and Paik's method the difference is yielding stress.

Table 4. Ultimate strength of bottom stiffened panels

| Design      | Method                                       |   |  |   |   |  |
|-------------|--|---|--|---|---|--|
|             | $\sigma_{xu}$ (MPa) Inner bottom without $p$ | $\sigma_{xu}$ (MPa) Inner bottom with $p = 0.359$ Mpa | $\sigma_{xu}$ (MPa) Outer bottom without $p$ | $\sigma_{xu}$ (MPa) Outer bottom with $p = 0.230$ Mpa | $\sigma_{xuP}$ (MPa) by Paik's FEA with $p = 0.160$ Mpa | $\sigma_{xuP}$ (MPa) by Paik's ALPS/ ULSAP |
| Pre-CSR     | 268.634                                      | 202.213   | 267.930                                      | 233.906   | 185.04  | 174.91                                     |
| CSR         | 267.684                                      | 196.494   | 267.324                                      | 228.194   | 198.12  | 195.74                                     |
| CSR/pre-CSR | 0.996  | 0.972   | 0.998  | 0.976   | 1.071   | 1.007                                      |

#### 4. CONCLUSIONS

The results of ultimate strength have just obtained by Nonlinear FEA with object ship VLOC, CSR and pre-CSR stiffened panel on deck and bottom. The comparison results in axial and biaxial on deck and bottom, respectively, with simply supported boundary condition, have designed by IACS pre-CSR and CSR under lateral pressure. There are three important conclusions of the ultimate strength assessment of the deck and bottom structures as follows.

1) The ultimate strength of deck stiffened-plate structures in cargo hold areas T-type is higher than L-type, i.e. 0.73-1.06 percent higher and 0.82-1.12 percent higher for CSR models and pre-CSR models, respectively. The difference between T-type and L-type is very small, and thus this can help the designers to make a good decision for appropriate requirements.

2) The bottom structural with appropriate choice of pre-CSR cross section model that can be obtained by Nonlinear FEA is better than CSR model at ultimate limit state, i.e. 0.23-2.50 percent higher and 0.35-2.91 percent higher in both outer bottom and inner bottom, respectively.

3) Total weight of the deck and bottom structures in the cargo hold areas by applying pre-CSR is about 640 tons (0.56 percent of hull structural weight) less than the structure designed by CSR. The ultimate strength of ship side structures is beyond the scope of our work and it will be studied in the future.

## ACKNOWLEDGEMENTS

The present study was undertaken at the School of Mechanical Science and Engineering, Huazhong University of Science and Technology, Wuhan, Hubei, 430074, P.R. China, which is a State Key Laboratory of Digital Manufacturing Equipment and Technology, Foundation NSFC No. 51235005, 973 program No. 2009CB724205.

## REFERENCES

- [1] O. F. Hughes, J. K. Paik, and D. Béghin, Ship structural analysis and design. Jersey City, N.J.: Society of Naval Architects and Marine Engineers, 2010.
- [2] IACS, Common Structural Rules for Bulk Carriers. London, UK: International Association of Classification Societies, 2006.
- [3] ABS, Rules for building and classing steel vessel. US: American Bureau of Shipping, 2012.
- [4] X. Z. Y. X.D. Chen, X.M. He, Xueming, T.H. Yan, "Dynamic characteristic analysis of precise long stroke linear motor with air-bearing in optical lithography," Chinese Journal of Mechanical Engineering (English Edition), vol. 21, pp. 17-22, 2008.
- [5] X. L. J. Lei, X.D. Chen, T.H. Yan, "Modeling and analysis of a 3-DOF Lorentz-force-driven planar motion stage for nanopositioning," Mechatronics, vol. 20, pp. 553-565, 2010.
- [6] X. Q. L. Z.X. Li, X.D. Chen, "The study on boundary conditions to the effect of mode analysis in FEA," China Mechanical Engineering, vol. 19, pp. 1083-1086, 2008.
- [7] H. K. K. Amlashi and T. Moan, "Ultimate strength analysis of a bulk carrier hull girder under alternate hold loading condition – A case study, Part 1: Nonlinear finite element modelling and ultimate hull girder capacity," Marine Structures, vol. 21, pp. 327-352, 2008.
- [8] H. K. K. Amlashi and T. Moan, "Ultimate strength analysis of a bulk carrier hull girder under alternate hold loading condition, Part 2: Stress distribution in the double bottom and simplified approaches," Marine Structures, vol. 22, pp. 522-544, 2009.
- [9] J. Keepaik, "Ultimate limit state performance of oil tanker structures designed by IACS common structural rules," Thin-Walled Structures, vol. 45, pp. 1022-1034, 2007.
- [10] M. Fujikubo, T. Yao, M. Khedmati, M. Harada, and D. Yanagihara, "Estimation of ultimate strength of continuous stiffened panel under combined transverse thrust and lateral pressure Part 1: Continuous plate," Marine Structures, vol. 18, pp. 383-410, 2005.
- [11] M. Fujikubo, M. Harada, T. Yao, M. Reza Khedmati, and D. Yanagihara, "Estimation of ultimate strength of continuous stiffened panel under combined transverse thrust and lateral pressure Part 2: Continuous stiffened panel," Marine Structures, vol. 18, pp. 411-427, 2005.
- [12] J. Choung, J.-M. Nam, and T.-B. Ha, "Assessment of residual ultimate strength of an asymmetrically damaged tanker considering rotational and translational shifts of neutral axis plane," Marine Structures, vol. 25, pp. 71-84, 2012.
- [13] J. K. Paik, B. J. Kim, and J. K. Seo, "Methods for ultimate limit state assessment of ships and ship-shaped offshore structures : Part I — Unstiffened plates," vol. 35, pp. 261-270, 2008.
- [14] J. K. Paik, B. J. Kim, and J. K. Seo, "Methods for ultimate limit state assessment of ships and ship-shaped offshore structures : Part II stiffened panels," vol. 35, pp. 271-280, 2008.
- [15] J. K. Paik, B. J. Kim, and J. K. Seo, "Methods for ultimate limit state assessment of ships and ship-shaped offshore structures: Part III hull girders," Ocean Engineering, vol. 35, pp. 281-286, 2008.
- [16] ISSC, "Ultimate strength," in 17th International Ship and Offshore structures Congress, Seoul Korea, 2009, pp. 375-474.
- [17] ISSC, "Ultimate strength," in 18th International Ship and Offshore structures Congress, Rostock Germany, 2012, pp. 285-363.
- [18] H. C. Do, W. Jiang, and J. X. Jin, "Estimation of Ultimate Limit State for Stiffened-Plates Structures: Applying for a Very Large Ore Carrier Structures Designed by IACS Common Structural Rules," Applied Mechanics and Materials, vol. 249-250, pp. 1012-1018, 2012.